



Design, Construction and Performance Evaluation of a Thermosyphon-Based Flat-Plate Solar Water Heater Using Locally Sourced Materials

Baba Shehu Abba Kawu¹, A.A. Safana², Ibrahim Murtala Musa², Mubarak Ibrahim²

¹Kashim Ibrahim University, Borno State, Nigeria.

²Federal University, Dutse, Department of Physics, Jigawa State, Nigeria.

Abstract

The increasing global demand for sustainable energy solutions necessitates the development of cost-effective renewable energy technologies, particularly in developing regions with abundant solar resources. This study presents the design, construction, and performance evaluation of a thermosyphon-based flat-plate solar water heater (SWH) fabricated entirely from locally sourced materials in Dutse, Jigawa State, Nigeria. The system comprises a flat-plate collector with a black-painted aluminum absorber plate, copper serpentine flow channels, a 3-litre cylindrical galvanized iron storage tank, a 4 mm transparent glass cover, and flexible plastic piping operating on the passive thermosyphon principle. Performance testing was conducted over six hours (10:00–15:00 hrs) under clear-sky ambient conditions at Federal University Dutse (latitude 9.08°N, longitude 7.40°E). Results demonstrated progressive water heating from an initial ambient temperature of 25°C to a peak outlet temperature of 65°C at 14:00 hours, representing a 40°C rise within four hours of operation. System efficiency varied from 4.28% to 100% throughout the testing period, with peak performance coinciding with maximum solar irradiance during midday hours. The thermosyphon principle enabled entirely pump-free operation, eliminating electricity requirements and reducing operational costs. This study demonstrates the technical feasibility and economic viability of locally manufactured solar water heaters for domestic applications in developing regions, contributing to reduced dependence on fossil fuels and promoting environmental sustainability.

Keywords: Solar Water Heater, Thermosyphon Principle, Flat-Plate Collector, Renewable Energy, Local Fabrication, Thermal Efficiency, Sustainable Technology.

INTRODUCTION

Global energy consumption patterns remain heavily dependent on fossil fuels, contributing significantly to greenhouse gas emissions, climate change, and environmental degradation (IPCC, 2021). The combustion of fossil fuels for energy production has resulted in unprecedented levels of atmospheric carbon dioxide, leading to global warming, extreme weather events, rising sea levels, and ecosystem disruption (Saidur et al., 2011). These environmental challenges have intensified the search for renewable, sustainable, and environmentally benign energy alternatives.

Solar energy represents one of the most promising renewable energy sources due to its abundance, accessibility, and minimal environmental impact. The sun delivers approximately 174 petawatts (1.74×10^{17} W) of solar radiation to Earth's upper atmosphere, far exceeding global human energy consumption (Union of Concerned Scientists,

2015). This vast energy potential can be harnessed through various technologies including photovoltaics for electricity generation and solar thermal systems for heat production. Solar water heating technology has emerged as a mature, cost-effective application of solar thermal energy for domestic and industrial purposes (Kalogirou, 2004).

The historical development of solar water heating traces back to ancient civilizations. Romans utilized solar heating concepts around 200 BCE to warm public baths, reducing fuel consumption and labor requirements (Gong & Sumathy, 2016). After centuries of dormancy, Swiss scientist Horace de Saussure reinvented the concept in 1767 by constructing an insulated box with glass panes and a black-painted bottom, demonstrating the greenhouse effect for the first time (Perlin, 2008). The first commercial solar water heater—the “Climax” system was patented by Clarence Kemp in 1891, featuring a combined collector-storage design. William J. Bailey revolutionized the technology in 1909 by separating

Citation: Baba Shehu Abba Kawu, A.A. Safana, et al., “Design, Construction and Performance Evaluation of a Thermosyphon-Based Flat-Plate Solar Water Heater Using Locally Sourced Materials”, Universal Library of Physics, 2026; 1(1): 05-10. DOI: <https://doi.org/10.70315/uloap.ulphy.2026.0101002>.

the collector and storage components and introducing the thermosyphon principle, enabling natural circulation without mechanical pumps (Gong & Sumathy, 2016).

Despite early promise, the solar water heating industry experienced a decline during the mid-20th century due to cheap fossil fuels. However, the 1970s oil crisis reignited global interest, and today the solar water heater market is valued at over one billion dollars with projected annual installations exceeding three million units by 2025 (Gupta, 2019). Solar radiation reaching Earth's surface varies significantly based on geographic location, atmospheric conditions, season, and time of day. Outside Earth's atmosphere, solar irradiance measures approximately $1,367 \text{ W/m}^2$, known as the solar constant (EIA, 2020). After atmospheric attenuation, average surface irradiance reduces to approximately $1,000 \text{ W/m}^2$ under clear-sky conditions. In Nigeria, northern regions demonstrate higher solar irradiance values compared to southern regions, attributed to proximity to the Sahara Desert and reduced cloud cover (Osinowo et al., 2015).

Nigeria faces significant energy challenges characterized by unreliable electricity supply, high dependence on fossil fuels, and limited access to modern energy services in rural areas. Electric water heaters, commonly used in urban areas, suffer from high operational costs and dependence on grid electricity. Solar water heating technology offers multiple benefits in this context: it reduces dependence on unreliable grid electricity, lowers long-term operational costs, eliminates greenhouse gas emissions from water heating, enables hot

water access in off-grid rural communities, and reduces foreign exchange expenditure through local fabrication.

Previous Nigerian research has demonstrated the feasibility of locally manufactured solar water heaters. Ogie et al. (2013) constructed a thermosyphon flat-plate system achieving a maximum outlet temperature of 55°C under $1,480 \text{ W/m}^2$ irradiance. Ekpo and Enyinna (2017) designed a system for 75 litres daily capacity at 60°C , achieving a peak outlet temperature of 76°C with a 2.3 m^2 collector area. The present study builds on this body of work by designing, constructing, and evaluating the performance of a portable thermosyphon-based flat-plate solar water heater using entirely locally sourced materials, with a focus on affordability, technical feasibility, and replicability for household-level deployment.

The thermosyphon principle, fundamental to passive systems, exploits density differences between hot and cold fluids. Solar radiation absorbed by the collector heats the working fluid, reducing its density and causing it to rise by natural convection into the storage tank positioned above. Simultaneously, cooler, denser fluid from the tank descends by gravity to the collector inlet, establishing continuous circulation without mechanical assistance (Ogie et al., 2013). The storage tank must be positioned at least 0.3–0.5 m above the collector to ensure adequate thermosyphon head, and the system is governed by well-established heat transfer and thermodynamic principles including energy conservation, the Stefan-Boltzmann radiation law, Fourier's law of conduction, and Newton's law of convective cooling.

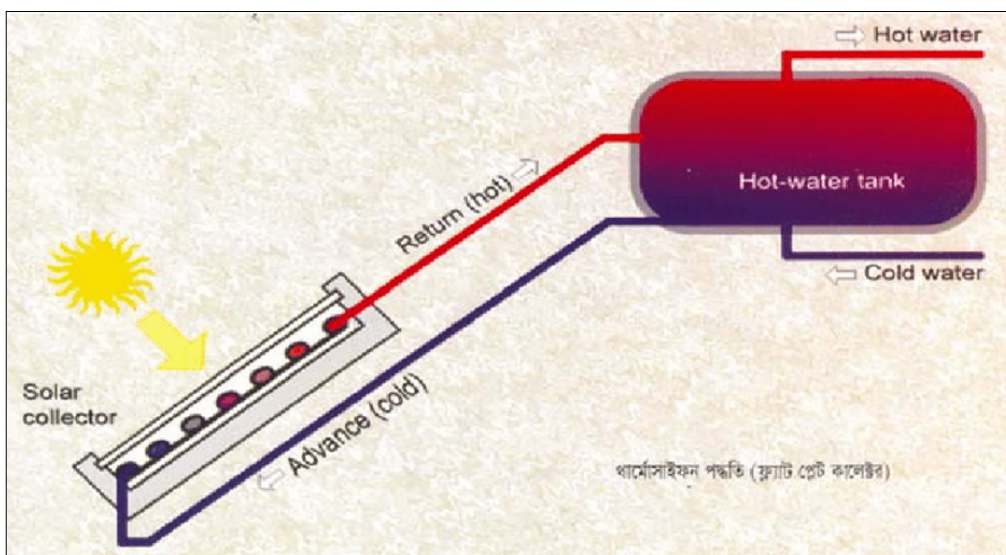


Figure 1. Thermosyphon solar heating system (Eschenbach, 2015)

MATERIALS AND METHODOLOGY

MATERIALS

1. Corrugated galvanized metal sheet of 1.2mm thickness
2. Aluminium
3. Copper pipe
4. Screw nail

5. Glass
6. Flexible pipe
7. Clips

The solar water heater was constructed using locally sourced materials available in Dutse, Jigawa State, Nigeria. The collector casing was fabricated from 1.2 mm corrugated galvanized iron sheet, cut and bent into a rectangular box

measuring 47.0 cm × 34.3 cm × 7.6 cm. The absorber plate consisted of a flat aluminum sheet coated with multiple layers of high-temperature black paint to enhance solar absorptivity ($\alpha \approx 0.92\text{--}0.96$), taking advantage of aluminum's relatively high thermal conductivity of approximately 237 W/mK.

The flow channels were fabricated from copper tubing (thermal conductivity ≈ 400 W/mK) bent into a serpentine pattern to maximize heat transfer surface area and secured to the absorber plate using aluminum wire to avoid thermal damage from welding. A 4 mm clear glass panel (44.5 cm × 33.0 cm) was mounted over the collector opening and secured with screw nails around the perimeter, providing high solar transmittance ($\tau \approx 0.90$) while minimizing convective and radiative losses from the absorber. The interior of the collector casing was painted black to reduce reflection losses.

The storage tank was fabricated from galvanized iron sheet, rolled and welded into a cylindrical shape with a capacity of 3 litres, suitable for a portable demonstration prototype. All internal seams were sealed with Top Bond adhesive to prevent leakage, and brass fittings were welded at the inlet (bottom) and outlet (top) positions to accommodate thermosyphon flow. The collector outlet was connected to the top of the tank, and the tank outlet to the bottom of the collector, using flexible plastic pipes secured with metal clips. The entire system was mounted on a metal frame oriented true south with a tilt angle of approximately 9°, corresponding to the site latitude, to maximize annual solar radiation collection (U.S. Department of Energy, 2012). The storage tank was positioned a minimum of 0.3 m above the top of the collector to ensure adequate thermosyphon head.

Performance testing was conducted at Federal University Dutse, Jigawa State, Nigeria (latitude 9.08°N, longitude 7.40°E) under clear-sky conditions. The tank was filled with 3 litres of tap water and mercury-in-glass thermometers were positioned at three locations: ambient air (shaded), collector inlet, and collector outlet (tank). Testing commenced at 10:00 hours and hourly temperature readings were recorded at 11:00, 12:00, 13:00, 14:00, and 15:00 hours, with thermometers allowed to stabilize for 2–3 minutes before each reading. Testing concluded at 15:00 hours after a six-hour observation period.

Instantaneous thermal efficiency was calculated using the expression:

$$\eta = [(T_{\text{out}} - T_{\text{in}}) / (T_{\text{max}} - T_{\text{in}})] \times 100\% \quad \dots (1)$$

where T_{out} is the measured outlet temperature, T_{in} is the initial inlet temperature, and T_{max} is the theoretical maximum temperature achievable, taken as the peak outlet temperature recorded during the test (65°C). This normalized efficiency metric expresses the ratio of actual to maximum achievable temperature rise under prevailing conditions. A more rigorous collector efficiency formulation would employ the Hottel-Whillier-Bliss equation:

$$\eta = FR[\tau\alpha - UL(T_{\text{in}} - T_{\text{amb}}) / IT] \quad \dots (2)$$

where FR is the heat removal factor, τ is glass transmittance, α is absorber absorptance, UL is the overall heat loss coefficient, and IT is total incident solar irradiance (Duffie & Beckman, 2013). Precise application of this equation was not possible in the current study due to the absence of calibrated pyranometer irradiance measurements and a flow meter, which are recommended for future investigations.

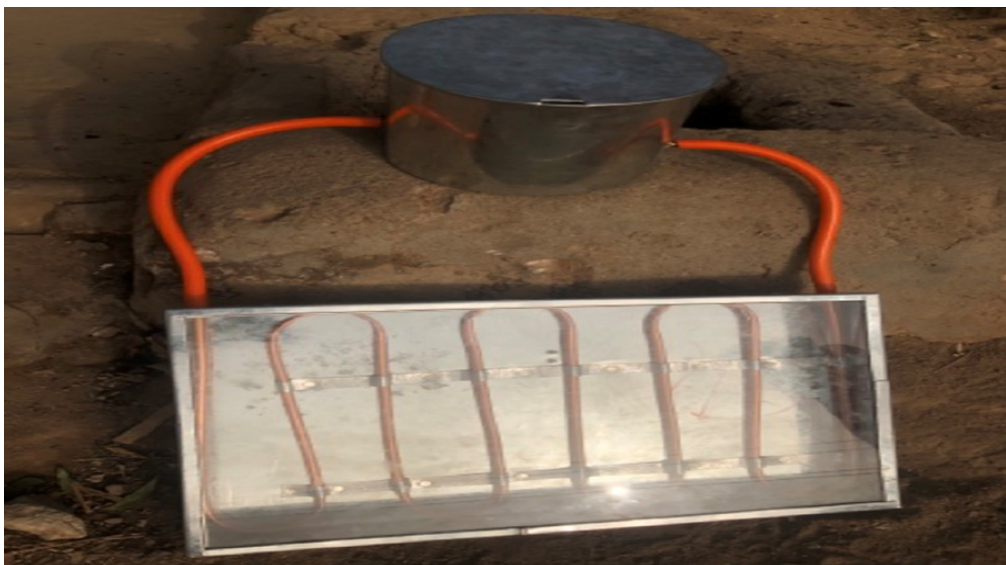


Figure 2. Solar water heater

RESULTS AND DISCUSSION

Table 1 presents the hourly temperature measurements and calculated efficiency values obtained during the six-hour testing period under clear-sky conditions. The system demonstrated a clear and progressive heating profile throughout the day, with water temperature rising from 27°C at 10:00 hours to a peak of 65°C at 14:00 hours, before declining to 37°C by 15:00 hours.

Table 1. Hourly Temperature Measurements and Calculated System Efficiency

Time (hrs)	Ambient Temp (°C)	Initial Temp (°C)	Final Temp (°C)	Temp Rise (°C)	Efficiency (%)
10:00	25.00	25.00	27.00	2.00	5.00
11:00	27.00	30.00	31.50	1.50	4.28
12:00	28.00	30.00	33.10	3.10	8.85
13:00	28.00	32.00	50.00	18.00	54.54
14:00	28.00	32.00	65.00	33.00	100.00
15:00	29.00	30.00	37.00	7.00	20.00

During the early morning period (10:00–12:00 hrs), system efficiency remained low, ranging from 4.28% to 8.85%. This is attributable to the thermal inertia of the collector components requiring initial energy input before effective heating commences, lower solar elevation angles producing reduced irradiance levels, and a temperature differential between the collector and tank that was insufficient to drive vigorous thermosyphon circulation. The modest temperature rise of only 1.5°C recorded at 11:00 hours is consistent with these compounding effects.

A marked acceleration in heating occurred between 12:00 and 13:00 hours, when the outlet temperature jumped from 33.10°C to 50.00°C—a rise of nearly 17°C within a single hour. This threshold behavior reflects the onset of robust thermosyphon circulation as the density differential between the heated collector fluid and the cooler tank water became sufficiently large to drive meaningful convective flow. As water in the collector absorbs heat, its density decreases according to $\rho_{hot} = \rho_{cold} / [1 + \beta(T_{hot} - T_{cold})]$, where $\beta \approx 0.000214 \text{ K}^{-1}$ for water at 20°C, generating the buoyancy-driven flow that underpins pump-free circulation. This positive feedback mechanism where greater temperature difference leads to stronger circulation and more efficient heat delivery explains the nonlinear temperature progression observed.

Peak performance was achieved at 14:00 hours, with an outlet temperature of 65°C representing a 40°C rise from initial ambient conditions. This temperature is well suited to domestic applications including bathing and personal hygiene (optimal 40–45°C), dishwashing (50–60°C), and laundry (50–55°C). The effective absorptance-transmittance product ($\tau\alpha$) of approximately 0.81–0.86, a consequence of the glass transmittance ($\tau \approx 0.90$) and the black-painted aluminum absorber ($\alpha \approx 0.92$ –0.96), ensured that a high fraction of incident solar radiation was captured and converted to thermal energy. High thermal conductivity of both the aluminum absorber (237 W/mK) and copper flow channels (400 W/mK) minimized thermal resistance in the conduction pathway from absorber surface to working fluid.

By 15:00 hours, the outlet temperature had dropped sharply to 37°C despite continued solar exposure. This decline is explained by the decreasing solar elevation angle in the late afternoon, which reduces both direct and diffuse irradiance, combined with increasing heat losses from the uninsulated

storage tank to the surroundings. Heat loss through the tank surface can be estimated from $Q_{loss} = UA(T_{tank} - T_{amb})$, where $U \approx 6$ –10 W/m²K for an uninsulated galvanized metal tank in still air, indicating substantial thermal leakage when the tank-to-ambient temperature differential exceeds 35°C. The absence of insulation on both the storage tank and the collector back is identified as the most significant design limitation of the current prototype, and its rectification through the addition of 50–75 mm fiberglass or polyurethane foam insulation is the highest-priority recommended improvement.

The peak outlet temperature of 65°C compares favorably with Ogie et al. (2013), who reported 55°C under 1,480 W/m² irradiance with a larger flat-plate thermosyphon system. While Ekpo and Enyinna (2017) achieved 76°C using a 2.3 m² collector area, their system was designed for 75-litre daily capacity with a substantially larger collector-to-storage ratio. The current study’s 65°C result with a compact 3-litre prototype underscores the importance of optimizing the collector-to-storage volume ratio rather than simply expanding collector area, as excessive aperture area without proportional insulation and storage improvements increases heat losses without commensurate temperature gains. The choice of black-painted aluminum over galvanized iron for the absorber plate is validated by Nshimyumuremyi and Junqi (2019), who demonstrated substantially improved efficiency upon this substitution, citing the superior thermal conductivity of aluminum (237 W/mK versus ~50 W/mK for galvanized iron).

International studies report flat-plate collector instantaneous efficiencies ranging from 30–70% depending on operating conditions and design quality (Kalogirou, 2004; Duffie & Beckman, 2013). The efficiency values reported in the present study, calculated as a normalized temperature-rise ratio rather than as a fraction of incident irradiance, are not directly comparable to these figures. The 100% value at 14:00 hrs indicates only that the system achieved its maximum observed temperature rise under the prevailing conditions, not thermodynamic impossibility. Future studies employing calibrated pyranometers and flow meters will enable calculation of standard collector efficiency using the Hottel-Whillier-Bliss formulation, permitting rigorous comparison with international benchmarks.

From an environmental perspective, replacing a conventional

electric water heater with this solar system eliminates approximately 633 kg of CO₂ emissions annually equivalent to 9.5 metric tons over the system's 15-year life based on Nigeria's grid carbon intensity of approximately 0.59 kg CO₂/kWh. Scaling to 10,000 households would eliminate roughly 6,460 metric tons of CO₂ per year, equivalent to removing approximately 1,400 passenger vehicles from roads. These figures, combined with the absence of operational air pollutants such as NO_x, SO₂, and particulate matter, underscore the meaningful contribution that widespread solar water heater adoption could make to Nigeria's climate commitments under the Paris Agreement.

Several limitations of the current study must be acknowledged. The 3-litre storage capacity is insufficient for practical household application, where 100–200 litres are typically required for a family. The lack of storage tank and collector back insulation led to significant heat losses and rapid afternoon temperature decline. Single-day testing under exclusively clear-sky conditions does not capture seasonal performance variation, particularly the reduced effectiveness expected during the rainy season (April–October) and during Harmattan dust events (December–February), when glass transmittance may be degraded by particulate deposition. The absence of calibrated pyranometer measurements and a flow meter precluded rigorous efficiency characterization. Future work should address these limitations through insulated scale-up designs, year-round performance monitoring across Nigeria's climatic zones, and full instrumentation for detailed thermal analysis.

CONCLUSION

This study successfully designed, constructed, and evaluated the performance of a thermosyphon-based flat-plate solar water heater fabricated from locally sourced materials in Dutse, Nigeria. The system achieved a peak outlet temperature of 65°C under clear-sky conditions, representing a 40°C rise from initial ambient temperature within four hours of operation. The thermosyphon mechanism proved effective in establishing natural convective circulation without any electrical input, with the characteristic nonlinear heating profile, marked by a dramatic temperature acceleration between 12:00 and 14:00 hours, confirming robust thermosyphon behavior during peak irradiance.

The system's zero operational electricity consumption translates to annual CO₂ savings of approximately 633 kg, contributing meaningfully to both household energy security and national climate commitments. All materials were procured locally, fabrication required only basic metalworking skills, and no imported components were necessary, demonstrating a replicable model for technology self-reliance applicable across developing regions with similar solar resources.

The primary design limitation identified is the absence

of storage tank, collector back, and pipe insulation, which caused significant afternoon heat loss and precludes overnight hot water availability. Addressing this through 50–75 mm fiberglass or polyurethane foam insulation is the highest-priority recommended improvement and would substantially extend hot water availability into evening hours. Scaling the system to 100–200 litre storage capacity with a 2–3 m² collector aperture, the addition of selective surface coatings on the absorber plate, and double-glazed collector covers are recommended enhancements for household-scale deployment.

REFERENCES

1. Adefarati, T., & Bansal, R.C. (2019). Energizing renewable energy systems and distribution generation. In *Pathways to a Smarter Power System* (pp. 29–65). Elsevier. <https://doi.org/10.1016/b978-0-08-102592-5.00002-8>
2. Alternative Energy Tutorials. (2015). Solar flat plate collectors for solar hot water. <http://www.alternative-energy-tutorials.com/solar-hot-water/flat-plate-collector.html>
3. Atia, D.M., Fahmy, F.H., Ahmed, N.M., & Dorrah, H.T. (2012). Optimal sizing of a solar water heating system based on a genetic algorithm for an aquaculture system. *Mathematical and Computer Modelling*, 55(3–4), 1436–1449. <https://doi.org/10.1016/j.mcm.2011.10.022>
4. Çengel, Y.A., & Ghajar, A.J. (2015). *Heat and Mass Transfer: Fundamentals and Applications* (5th ed.). McGraw-Hill Education.
5. Duffie, J.A., & Beckman, W.A. (2013). *Solar Engineering of Thermal Processes* (4th ed.). John Wiley & Sons.
6. Ekpo, J., & Enyinna, P. (2017). Design and construction of a solar water heater for environmental sustainability. *British Journal of Applied Science & Technology*, 20(3), 1–15. <https://doi.org/10.9734/bjast/2017/31820>
7. Energy Information Administration (EIA). (2020). Where solar is found. <https://www.eia.gov/energyexplained/solar/where-solar-is-found.php>
8. Gong, J., & Sumathy, K. (2016). Active solar water heating systems. In *Advances in Solar Heating and Cooling* (pp. 191–210). Elsevier. <https://doi.org/10.1016/B978-0-08-100301-5.00009-6>
9. Gupta, A. (2019). Solar water heater market trends 2019–2025: Industry share forecast. *Global Market Insights*. <https://www.gminsights.com/industry-analysis/solar-water-heater-market>
10. Hasan, A. (1997). Thermosyphon solar water heaters: Effect of storage tank volume and configuration on efficiency. *Energy Conversion and Management*, 38(9), 847–854. [https://doi.org/10.1016/S0196-8904\(96\)00099-4](https://doi.org/10.1016/S0196-8904(96)00099-4)

11. Ineichen, P., Guisan, O., & Perez, R. (1990). Ground-reflected radiation and albedo. *Solar Energy*, 44(4), 207–214. [https://doi.org/10.1016/0038-092X\(90\)90149-7](https://doi.org/10.1016/0038-092X(90)90149-7)
12. IPCC. (2021). *Climate Change 2021: The Physical Science Basis. Contribution of Working Group I to the Sixth Assessment Report of the Intergovernmental Panel on Climate Change*. Cambridge University Press.
13. Kalogirou, S.A. (2004). Solar thermal collectors and applications. *Progress in Energy and Combustion Science*, 30(3), 231–295. <https://doi.org/10.1016/j.pecs.2004.02.001>
14. Lilian, I.N., Daniel, O., & Joseph, O. (2018). Modelling the solar radiation parameter over Abuja using neural networks. *Journal of Applied Sciences and Environmental Management*, 22(5), 697–702.
15. Nshimyumuremyi, E., & Junqi, W. (2019). Thermal efficiency and cost analysis of solar water heater made in Rwanda. *Energy Exploration and Exploitation*, 37(3), 1147–1161. <https://doi.org/10.1177/0144598718815240>
16. Ogie, N.A., Oghogho, I., & Jesumirewhe, J. (2013). Design and construction of a solar water heater based on the thermosyphon principle. *Journal of Fundamentals of Renewable Energy and Applications*, 3, 1–8. <https://doi.org/10.4303/jfrea/235592>
17. Osinowo, A.A., Okogbue, E.C., Ogungbenro, S.B., & Fashanu, O. (2015). Analysis of global solar irradiance over climatic zones in Nigeria for solar energy applications. *Journal of Solar Energy*, 2015, 1–9. <https://doi.org/10.1155/2015/819307>
18. Perlin, J. (2008). Workhorse of the solar industry. *Pacific Standard*. <https://psmag.com/environment/workhorse-of-the-solar-industry-4736>
19. Saidur, R., Abdelaziz, E.A., Demirbas, A., Hossain, M.S., & Mekhilef, S. (2011). A review on biomass as a fuel for boilers. *Renewable and Sustainable Energy Reviews*, 15(5), 2262–2289. <https://doi.org/10.1016/j.rser.2011.02.015>
20. Union of Concerned Scientists. (2015). The solar resource. <https://www.ucsusa.org/resources/solar-resource>
21. U.S. Department of Energy. (2012). Solar water heaters. <https://www.energy.gov/energysaver/water-heating/solar-water-heaters>
22. Zeghib, I., & Chaker, A. (2011). Simulation of a solar domestic water heating system. *Energy Procedia*, 6, 292–301. <https://doi.org/10.1016/j.egypro.2011.05.033>